Synthesis, Characterization, and Redox Behavior of Mixed 1,3-Diyne Dicobalt/Triosmium and Dicobalt/Triruthenium Carbonyl Clusters

Consuelo Moreno,*[,†] María-Luisa Marcos,[‡] María-José Macazaga,[†] Javier Gómez-González,[†] Raquel Gracia,[†] Fernando Benito-López,[†] Esther Martínez-Gimeno,[†] Avelina Arnanz,[†] Manuela-Eloisa Medina,[§] César Pastor,[§] Jaime González-Velasco,[‡] and Rosa-María Medina[†]

Departamento de Química Inorgánica de la Universidad Autónoma de Madrid, Departamento de Química de la Universidad Autónoma de Madrid, and Servicio Interdepartamental de Investigación de la Facultad de Ciencias de la Universidad Autónoma de Madrid, 28049 Madrid, Spain

Received May 28, 2007

The reaction between $[Co_2(\mu-\eta^2\text{-}HC{\equiv}CC_2SiMe_3)(\mu\text{-dmpm})(CO)_4]$ (**1**) and $[Os_3(CO)_{10}(MeCN)_2]$ gives rise to the formation of three new products: $[Os_3(\mu\text{-H})\{\mu_3\text{-}\eta^1{:}\eta^2;\mu\text{-}\eta^2\text{-}C_2C_2SiMe_3[Co_2(\mu\text{-dmpm})(CO)_4]\}(CO)_9]$ (**3**), $[Os_3(\mu\text{-H})\{\mu\text{-}\eta^1;\mu\text{-}\eta^2\text{-}C_2C_2SiMe_3[Co_2(\mu\text{-dmpm})(CO)_4]\}(CO)_{10}]$ (**4**), and $[Os_3\{\mu_3\text{-}\eta^1{:}\eta^2;\mu\text{-}\eta^2\text{-}HC_2C_2SiMe_3[Co_2(\mu\text{-dmpm})(CO)_4]\}(\mu\text{-CO})(CO)_9]$ (**5**). These complexes adopt three different coordination modes: $\mu_3\text{-}\eta^2$ perpendicular, $\mu\text{-}\eta^1$ edge-bridged, and $\mu_3\text{-}\eta^2$ parallel mode, respectively. When the reaction is carried out with $[Ru_3(CO)_{12}]$, only one product is obtained, $[Ru_3(\mu\text{-H})\{\mu_3\text{-}\eta^1{:}\eta^2;\mu\text{-}\eta^2\text{-}C_2C_2SiMe_3[Co_2(\mu\text{-dmpm})(CO)_4]\}(CO)_9]$ (**6**), in which the triruthenium cluster is coordinated in a perpendicular mode. However, the reaction of $[Co_2(\mu\text{-}\eta^2\text{-}HC_2(C{\equiv}C)_2C_2SiMe_3)(\mu\text{-dppm})(CO)_4]$ (**2**), stericaly more congested, with $[Os_3(CO)_{10}(Me_3CN)_2]$ yields only one product, the edge-bridged-coordinated $[Os_3(\mu\text{-H})\{\mu\text{-}\eta^1;\mu\text{-}\eta^2\text{-}C_2C_2SiMe_3[Co_2(\mu\text{-dppm})(CO)_4]\}(CO)_{10}]$ (**7**). $[Os_3(CO)_{10}(MeCN)_2]$ reacts with $HC{\equiv}CSiMe_3$, giving rise to the known parallel and perpendicular complexes and the new edge-bridged $[Os_3(\mu\text{-H})\{\mu\text{-}\eta^1\text{-}C_2SiMe_3\text{-}(CO)_{10}]$. All products were characterized by analytical and spectroscopic data (IR, ^1H, ^{13}C, and ^{31}P NMR, and MS). Crystals of **3**, **6**, and **7** suitable for single-crystal X-ray diffraction were grown, and the molecular structures of these compounds are discussed. A comparative electrochemical study of all these complexes is presented by means of the cyclic and square-wave voltammetry techniques.

Introduction

The chemistry of alkynes coordinated to transition metals has been extensively studied and is well established.[1] The current interest in these kinds of complexes is partially due to the stabilizing influence of the metal on reactive unsaturated carbon chains and polycarbon ligands[1,2] and the potential properties of such compounds as nonlinear optical materials[3] and as "molecular" wires.[4,5] As these properties are due mainly to their linear structure, high stability, and π-electronic conjugation, alkynyl or polyynediyl bridging ligands have been shown to be especially efficient in allowing the passage of electronic effects between redox active centers,[5k,6] and therefore their electronic properties can be modified by changing metal fragments and/or alkyne ligands.[7] Transition metal clusters should function well as electron reservoirs, capable of both accepting and releasing electrons,[8] and as such these species may find some use in the construction of nanoscale electronic circuits.[9] The electronic communication through such potential molecular wires is often evaluated by examinating the redox response of electroactive groups.[10]

* To whom correspondence should be addressed. E-mail: mconsuelo.moreno@uam.es.

† Departamento de Química Inorgánica.

‡ Departamento de Química.

§ Servicio Interdepartamental de Investigación de la Facultad de Ciencias.

(1) (a) Sapa, A.; Tiripicchio, A.; Braunstein, P. *Chem. Rev.* **1983**, *83*, 203. (b) Rainthby, P. R.; Rosales, M. J. *Adv. Inorg. Chem. Radiochem.* **1985**, *29*, 169.

(2) (a) Diederich, F.; Rubin, Y. *Angew. Chem.* **1992**, *104*, 1123. (b) Rubin, Y.; Knobler, C. B.; Diederich, F. *J. Am. Chem. Soc.* **1990**, *112*, 4966. (c) Diederich, F.; Rubin, Y.; Chapman, O. L.; Goroff, N. S. *Helv. Chim. Acta* **1994**, *77*, 1441. (d) Rappert, T.; Nürnberg, O.; Werner, H. *Organometallics* **1993**, *12*, 1359. (e) Werner, H.; Gevert, O.; Steinert, P.; Wolf, J. *Organometallics* **1995**, *14*, 1786. (f) Lewis, J.; Lin, B.; Khan, M. S.; Al-Mandhary, M. R. A.; Raithby, P. R. *J. Organomet. Chem.* **1994**, *484*, 161.

(3) (a) Green, M. L. H.; Marder, S. R.; Thomson, M. E.; Bandy, J. A.; Bloor, D.; Kolomsky, P. V.; Jones, R. J. *Nature* **1987**, *330*, 360. (b) Hunter, A. D. *Organometallics* **1989**, *8*, 1118. (c) Chukwu, R.; Hunter, A. D.; Santarsiero, B. D. *Organometallics* **1992**, *11*, 589. (d) Yuan, Z.; Taylor, N. J.; Sun, Y.; Marder, T. B.; Williams, I. D.; Cheng, J. T. *J. Organomet. Chem.* **1993**, *449*, 27. (e) Beck, W.; Niemer, B.; Wieser, M. *Angew. Chem., Int. Ed. Engl.* **1994**, *33*, 385.

(4) (a) Creager, S.; Yu, C. J.; Bamdad, C.; O'Connor, S.; Maclean, T.; Lam, E.; Chong, Y.; Olsen, G. T.; Luo, J.; Gozon, M.; Hayyem, J. F. *J. Am. Chem. Soc.* **1999**, *121*, 1059. (b) Stepnicka, P.; Gyepes, R.; Císarova, I. *Organometallics* **1999**, *18*, 627. (c) Dosa, P. I.; Erben, C.; Iyer, V. S.; Vollhardt, K. P. C.; Wasser, I. M. *J. Am. Chem. Soc.* **1999**, *121*, 10430. (d) McQuade, D. T.; Pullen, A. E.; Swager, T. M. *Chem. Rev.* **2000**, *100*, 2537. (e) Roncali, J. *Chem. Rev.* **1997**, *97*, 173.

(5) (a) Birge, R. R., Ed. *Molecular and Biomolecular Electronics; Advances in Chemistry Series 240*; American Chemical Society: Washington, CD, 1991. (b) Kirk, W. P., Reed, M. A. Eds. *Nanostructures and Mesoscopic Systems*; Academic: New York, 1992. (c) Aviram, A., Ed. *Molecular Electronics: Science and Technology; Confer. Proc. No. 262*; American Institute of Physics: New York, 1992. (d) Astruc, D. *Electron Transfer and Radical Processes in Transition-metal Chemistry*; VCH Publishers: New York, 1995. (e) Ward, M. D. *Chem. Soc. Rev.* **1995**, 121. (f) Andres, R. P.; Bielefeld, J. D.; Henderson, J. I.; Janes, D. B.; Kolagunta, V. R.; Kubiak, C. P.; Mahoney, W. J.; Osifchin, R. G. *Science* **1996**, *273*, 1690. (g) Grosshenny, V.; Harriman, A.; Hissler, M.; Ziessel, R. *Plat. Met. Rev.* **1996**, *40*, 26. (h) Grosshenny, V.; Harriman, A.; Hissler, M.; Ziessel, R. *Plat. Met. Rev.* **1996**, *40*, 72. (i) Barlow, S.; O'Hare, D. *Chem. Rev.* **1997**, *97*, 637. (j) Feldheim, D.; Keating, C. D. *Chem. Soc. Rev.* **1998**, *27*, 1. (k) Paul, F.; Lapinte, C. *Coord. Chem. Rev.* **1998**, *431*, 178−180, (l) Collier, C. P.; Wong, E. W.; Belohradsky, M.; Raymo, F. M.; Stoddart, J. F.; Kuekes, P. J.; Williams, R. S.; Heath, J. R. *Science* **1999**, *285*, 391. (m) Kheradmandan, S.; Heinze, K.; Schmalle, H. W.; Berke, H. *Angew. Chem., Int. Ed.* **1999**, *38*, 2270.

10.1021/om700525z CCC: $37.00
Publication on Web 09/14/2007

In addition, the redox properties of mixed transition metal−main group cluster cores have also attracted a great deal of attention in their own right, as these compounds play a crucial role in biological electron transport cycles.[11] Therefore compounds in which multinuclear cluster cores are linked by polyynyl ligands would appear to have great potential for use in construction of large electroactive molecular assemblies.

The wide variety of metal coordination modes to alkyne ligands is well established and constitutes a fundamental part of every textbook on organometallic chemistry.[12] The coordination mode of an alkyne to metal clusters has been shown to be dependent on both the metal and the substituents on the alkyne.[13]

Thus, the reactions of terminal alkynes, HC≡CR, with trinuclear metal clusters such as $[Os_3(CO)_{10}(MeCN)_2]$ give the triply bridging alkyne compounds $[Os_3(\mu_3\text{-}\eta^2\text{-alkyne})(CO)_{10}]$, which often lead to hydrogen transfer to the metal, giving $[Os_3H(\mu_3\text{-}\eta^2\text{-alkyne})(CO)_9]$, where the unsaturation resulting from the loss of CO is compensated by oxidative addition with C−H bond cleavage.[14] With RC≡CR type alkynes either a perpendicular $\mu_3\text{-}\eta^2$ (⊥) mode or, more commonly, a parallel $\mu_3\text{-}\eta^2$ (∥) mode of coordination is observed. Thus, the perpendicular coordination mode is found in 46-electron clusters, while the parallel one is observed to be present in 48-electron clusters.[13c,15]

The 1,3-diynes RC≡CC≡CR (R = Me, Et, Ph, $SiMe_3$, etc.) react at room temperature with $[Os_3(CO)_{10}(MeCN)_2]$ to give the clusters $[Os_3(\mu_3\text{-}\eta^2\text{-}R_2C_4)(\mu\text{-CO})(CO)_{10}]$ in which only one of the alkyne groups is coordinated. In all cases clusters decarbonylate thermally to $[Os_3(\mu_3\text{-}\eta^2\text{-alkyne})(CO)_9]$, but the nature of these species depends on R. When there are no C−H α-bonds in the diyne, the major product is $[Os_3(\mu\text{-}\eta^2\text{-C}\equiv\text{CR})_2(CO)_9]$, resulting from the cleavage of the central carbon−carbon bond of the diyne, but C−H cleavage is favored if α-bonds are present.[16]

Like many other groups we were attracted by the architectural versatility of trimetallic clusters, which should allow many different modes of chain−carbon attachment, by the possibility to change the coordination mode of the alkyne by electrochemical techniques, and by the possibility to obtain modified electrodes. Thus, in this paper, we report the synthesis, characterization, and the redox properties of several complexes containing 1,3-diyne, "Co_2", and "Ru_3" or "Os_3" units.

Results and Discussion

Synthesis of σ- and π-Acetylenic Complexes. The bis-acetonitrile complexes $[M_3(CO)_{10}(MeCN)_2]$ (M = Os, Ru) have been established as convenient precursors in the preparation of carbonyl alkyne clusters.[17] In order to form mixed "Co_2Os_3" and "Co_2Ru_3" complexes, we have used the uncoordinated −C≡CH portion of compounds **1** and **2**. Thus reaction of $[Co_2(\mu\text{-}\eta^2\text{-HC}\equiv\text{CC}_2SiMe_3)(\mu\text{-dmpm})(CO)_4]$ (**1**) with $[Os_3(CO)_{10}(MeCN)_2]$, in CH_2Cl_2, at room temperature for 26 h, affords three new compounds (**3**−**5**) (Scheme 1) after separation and purification by TLC plates using hexane/CH_2Cl_2 (3:1) as eluent. The main, dark red-brown, air-stable product **4**, with an edge-bridging coordination, was obtained in 52% yield (medium R_f) and was characterized as $[Os_3(\mu\text{-H})\{\mu\text{-}\eta^1\text{:}\mu\text{-}\eta^2\text{-C}_2C_2SiMe_3[Co_2(\mu\text{-dmpm})(CO)_4]\}(CO)_{10}]$, by spectroscopic methods (see Experimental Section). The second product, **5**, was obtained as a brownish-yellow solid in 33% yield (low R_f) and was characterized by spectroscopic methods as $[Os_3\{\mu_3\text{-}\eta^1\text{:}\eta^2\text{;}\mu\text{-}\eta^2\text{-HC}_2C_2SiMe_3[Co_2(\mu\text{-dmpm})(CO)_4]\}(\mu\text{-CO})(CO)_9]$. Complex **3**, $[Os_3(\mu\text{-H})\{\mu_3\text{-}\eta^1\text{:}\eta^2\text{;}\mu\text{-}\eta^2\text{-C}_2C_2SiMe_3[Co_2(\mu\text{-dmpm})(CO)_4]\}(CO)_9]$, was obtained in 15% yield (high R_f) and was characterized by spectroscopic and crystallographic methods. At room temperature **5** is slowly transformed into the acetylide compound **3**. Therefore **3** can be prepared by heating a hexane solution of the parallel derivative **5**.

The stabilization of ruthenium systems containing terminal alkynes coordinated in a perpendicular mode seems to be preferred over that of corresponding osmium systems. This coordination mode is stabilized by back-donation from the metal atoms to the alkyne.[13c,15c,d] Therefore, reaction of **1** with $[Ru_3(CO)_{10}(MeCN)_2]$ or $[Ru_3(CO)_{12}]$ in CH_2Cl_2/MeCN at room temperature for 48 h affords only one product, the stable brown-yellow solid **6**, in a 80% yield after purification by TLC using hexane/CH_2Cl_2 (1:1) as eluent. The product was characterized

(6) (a) Le Narvor, N.; Toupet, L.; Lapinte, C. *J. Am. Chem. Soc.* **1995**, *117*, 7129. (b) Bartik, T.; Bartik, B.; Dembinski, R.; Gladysz, J. A. *Angew. Chem., Int. Ed. Engl.* **1996**, *35*, 414. (c) Coat, F.; Lapinte, C. *Organometallics* **1996**, *15*, 477. (d) Jung, T. S.; Kim, J. H.; Jang, E. K.; Kim, D. H.; Sim, Y.-B.; Park, B.; Shin, S. C. *J. Organomet. Chem.* **2000**, *599*, 232. (e) Moreno, C.; Marcos, M. L.; Domínguez, G.; Arnanz, A.; Farrar, D. H.; Teeple, R.; Lough, A.; González-Velasco, J.; Delgado, S. *J. Organomet. Chem.* **2001**, *631*, 19. (f) Adams, R. D.; Qu B. *Organometallics* **2000**, *19*, 2411. (g) Marcos, M. L.; Macazaga, M. J.; Medina, R. M.; Moreno, C.; Castro, J. A.; Gomez, J. L.; Delgado, S.; González-Velasco, J. *Inorg. Chim. Acta* **2001**, *312*, 249. (h) Medina, R. M.; Moreno, C.; Marcos, M. L.; Castro, J. A.; Benito, F.; Arnanz, A.; Delgado, S.; González-Velasco, J.; Macazaga, M. J. *Inorg. Chim. Acta* **2004**, *357*, 2069. (i) Macazaga, M. J.; Marcos, M. L.; Moreno, C.; Benito-Lopez, F.; Gómez-Gonzalez, J.; González-Velasco, J.; Medina, R. M. *J. Organomet. Chem.*, unpublished work.

(7) (a) Roncali, J. *Chem. Rev.* **1997**, *97*, 173. (b) McQuade, D. T.; Pullen A. E.; Swager, T. M. *Chem. Rev.* **2000**, *100*, 2537. (b) Low, P. J.; Bruce, M. I. *Adv. Organomet. Chem.* **2002**, *48*, 71. (c) Bruce, M. I.; Low, P. J. *Adv. Organomet. Chem.* **2004**, *50*, 179.

(8) (a) Lemoine, P. *Coord. Chem. Rev.* **1982**, *47*, 56. (b) Lemoine, P. *Coord. Chem. Rev.* **1988**, *83*, 169. (c) Geiger, W. E. *Prog. Inorg. Chem.* **1985**, *33*, 275. (d) Drake, S. R. *Polyhedron* **1990**, *9*, 455. (e) Low, P. J.; Rousseau, R.; Lam, P.; Udachin, K. A.; Enright, G. D.; Tse, J. S.; Wayner, D. D. M.; Carty, A. J. *Organometllics* **1999**, *18*, 3885.

(9) Andres, R. P.; Bielefeld, J. D.; Henderson, J. I.; Janes, D. B.; Kolagunta, V. R.; Kubiak, C. P.; Mahoney, W. J.; Osifchin, R. G. *Science* **1996**, *273*, 1690.

(10) (a) Worth, G. H.; Robinson, B. H.; Simpson, J. *Appl. Organomet. Chem.* **1990**, *4*, 481. (b) Robinson, B. H. *Chemistry and Reactivity of Metal Cluster Carbonyl Radical Anions in Paramagnetic Organometallic Species in Activation, Selectivity and Catalysis*; Kluwer: Dordrecht, 1987. (c) Bard, A. J.; Faulkner, L. R. *Electrochemical Methods*; Wiley: New York, 1980. (d) Ward, M. D. *Chem. Soc. Rev.* **1995**, *24* (2), 121.

(11) (a) Goh, C.; Holm, R. H. *Inorg. Chim. Acta* **1998**, *270*, 46. (b) Noodlemen, L.; Peng, C. Y.; Case, D. A.; Mouesca, J.-M. *Coord. Chem. Rev.* **1995**, *144*, 199. (c) Golbeck, J. H. *Biochim. Biophys. Acta* **1987**, *895*, 167. (d) Cammack, R., Sykes, A. G., Eds. *Iron-Sulfur Proteins*; Academic Press: San Diego, 1992; and references therein.

(12) (a) Elschenbroich, C; Salzer, A. *Organometallics: a concise introduction*, 2nd ed.; VCH: Weinheim, 1992. (b) Crabtree, R. H. *The Organometallic Chemistry of the Transition Metals*, 4th ed.; Wiley-Interscience: Hoboken, NJ, 2005.

(13) (a) Sappa, E.; Tiripicchio, A.; Braunstein, P. *Chem. Rev.* **1983**, *83*, 203. (b) Osella, D.; Raithby, P. R. *Stereochemistry of Organometallic and Inorganic Compounds*; Bernal, I., Ed.; Elsevier: Amsterdam, 1988; Vol. 3. (c) Brown, M. P.; Dolby, P. A.; Harding, M. M.; Mathews, A. J.; Smith, A. K.; Osella, D.; Arbrun, M.; Gobetto, R.; Raithby, P. R.; Zanello, P. *J. Chem. Soc., Dalton Trans.* **1993**, 827. (d) Bruce, M. I.; Low, P. J.; Werth, A.; Skelton, B. W.; White, A. H. *J. Chem. Soc., Dalton Trans.* **1996**, 1551.

(14) (a) *Adv. Organomet. Chem.* **1986**, *26*, 1. (b) Deeming, A. J.; Hasso, S.; Underhill, M. *J. Chem. Soc., Dalton Trans.* **1975**, 1614.

(15) (a) Osella, D.; Gobetto, R.; Montenegro, P.; Zanello, P.; Cinquantini, A. *Organometallics* **1985**, *5*, 1247. (b) Schilling, B. E. R.; Hoffmann, R. *J. Am. Chem. Soc.* **1979**, *101*, 3456. (c) Granozzi, G.; Tondello, E.; Casarin, m.; Aime, S.; Osella, D. *Organometallics* **1983**, *2*, 430. (d) Aime, S.; Bertoncello, R.; Busetti, V.; gobetto, R.; Granozzi, G.; Osella, D. *Inorg. Chem.* **1986**, *25*, 4004.

(16) (a) Deeming, A. J.; Felix, M. S. B.; Nuel, D. *Inorg. Chim. Acta* **1993**, *213*, 3. (b) Adams R. D.; Qu, B.; Smith, M. D.; Albright T. A. *Organometallics* **2002**, *21*, 2970. (c) Zuno-Cruz, F. J.; Carrasco, A. L.; Rosales-Hoz, M. J. *Polyhedron* **2002**, *21*, 1105.

(17) Foulds, G. A.; Johnson, B. F. G.; Lewis, J. *J. Organomet. Chem.* **1985**, *296*, 147.

Scheme 1

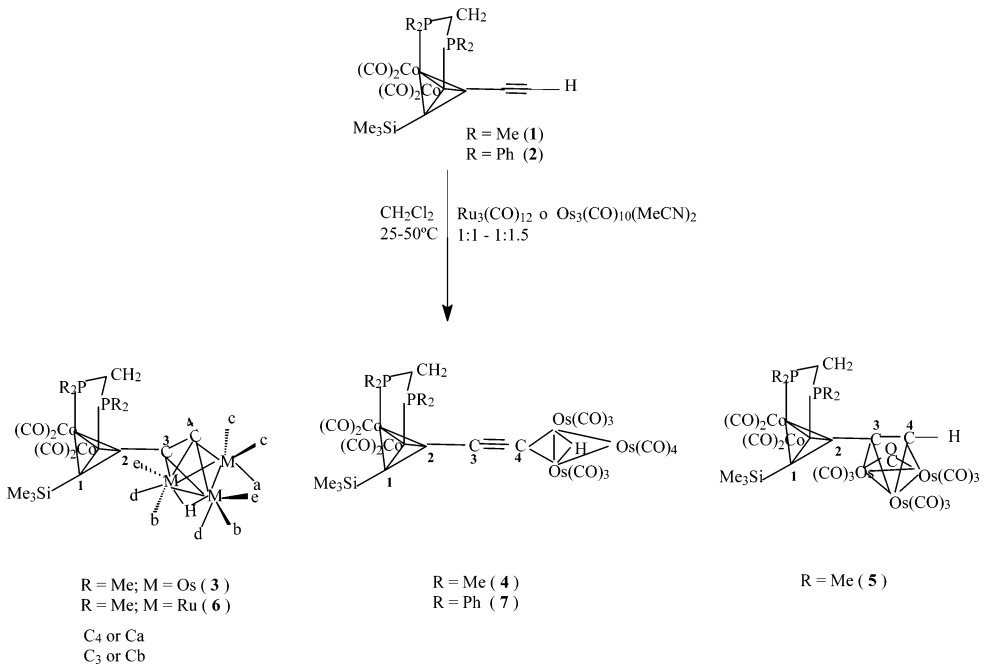

by spectroscopic and crystallographic methods as $[Ru_3(\mu\text{-H})\{\mu_3\text{-}\eta^1\text{:}\eta^2\text{;}\mu\text{-}\eta^2\text{-}C_2C_2SiMe_3[Co_2(\mu\text{-dmpm})(CO)_4]\}(CO)_9]$ (see Experimental Section).

In order to study the influence of the steric factors on the variety and coordination mode of the alkyne to the Os_3 cluster, we changed the dmpm ligand in **1** to a bulkier one, the dppm ligand. Thus the reaction of **2** (sterically more congested) with the "Os_3" cluster, under the same conditions, affords only one final product, **7**, with the $\mu\text{-}\eta^1$ edge-bridging coordination mode (Scheme 1). This dark red, air-stable product was obtained in 91% yield and was characterized as $[Os_3(\mu\text{-H})\{\mu\text{-}\eta^1\text{;}\mu\text{-}\eta^2\text{-}C_2C_2SiMe_3[Co_2(\mu\text{-dppm})(CO)_4]\}(CO)_{10}]$ by spectroscopic and crystallographic methods (see Experimental Section).

Although reactions of terminal alkynes and triangular metal clusters very often lead to hydrogen transfer to the metal core with formation of acetylide groups,[13c,16c] in our case complex **1**, containing a small phosphine ligand, reacts with the triosmium cluster, affording complexes **3**−**5**, with different coordination modes. Thus, while **3** presents the known perpendicular coordination mode, where the unsaturation resulting from the loss of CO is compensated by oxidative addition with C−H bond cleavage, complex **4**, like **7**, presents a novel coordination mode only found in "$Re(CC)_nOs_3$" mixed species,[18] where only the terminal carbon is σ-coordinated to two Os metals in an edge-bridged mode.

Cluster $[Os_3(CO)_{10}(CH_3CN)_2]$ reacts at room temperature with trimethylsilylacetylene to afford the new edge-bridged complex $[Os_3(\mu\text{-H})\{\mu\text{-}\eta^1\text{-}C_2SiMe_3(CO)_{10}]$ (**8**) in 12% yield, minor amounts of $[Os_3(\mu\text{-H})\{\mu_3\text{-}\eta^1\text{:}\eta^2\text{-}C_2SiMe_3(CO)_9]$ (**9**), and the known orange derivative $[Os_3\{\mu_3\text{-}\eta^1\text{:}\eta^2\text{-}HC_2SiMe_3(\mu\text{-CO})(CO)_9]$, which undergoes decarbonylation and hydrogen migration at high temperature to give the cluster **9**. These complexes were characterized by spectroscopic methods (see Experimental Section).

Spectroscopic Characterization of σ- and π-Acetylenic Complexes. All these compounds have been characterized by analytical and spectroscopic data (IR, ^1H, $^1H\{^{31}P\}$, ^{13}C, and ^{31}P NMR, MS, and X-ray crystallography), details of which are given in the Experimental Section. The IR spectra of **3**−**7** exhibit six strong absorptions in the terminal carbonyl stretching region at 2100−1960 cm^{-1}, and the spectral patterns are similar to those observed for previously reported dicobalt-triosmium and dicobalt-triruthenium-alkyne complexes.[13b−d,16a−c,18] In addition complexes **4** and **7** present a weak $\nu(C{\equiv}C)$ absorption at ca. 2143 cm^{-1}. As expected, very little difference is observed in the frequency values for the terminal CO stretching bands from one coordination mode to the other. The IR spectrum of **8** exhibits six strong absorptions in the carbonyl stretching region at 2100−1960 cm^{-1}, and data for compounds already described (**9** and **10**) agree with those reported.[19]

However, large differences are observed in the NMR results. Thus, ^1H chemical shifts for different coordination modes appear at very different fields. The ^1H NMR spectra of compounds **3**, **4**, **6**, **7**, and **8** show the presence of a hydride group: for acetylide perpendicular complexes **3** and **6** at ca. −22 ppm and for edge-bridged **4**, **7**, and **8** at ca. −16 ppm. These values are in the same range as those observed in other $\mu_3\text{-}\eta^2$ perpendicular[16c,20] and $\mu\text{-}\eta^1$ edge-bridged[18] compounds. Compounds **3**, **4**, **7**, and **8** show the presence of satellites due to $^{187}Os-^1H$ coupling with J values of 16.1 Hz for $\mu_3\text{-}\eta^2$ perpendicular mode (**3**) and ca. 17.5 Hz for $\mu\text{-}\eta^1$ edge-bridged mode (**4**, **7**, **8**). These values are in the same range as those observed in other μ_2-hydride groups.[20,21]

An alkyne derivative proton NMR spectrum shows that the chemical shift for the CH group moves significantly downfield (8.78 ppm) in the coordinated parallel complex **5** in comparison with the shift observed in the parent complex **1** (3.45 ppm).

In addition, in the ^1H NMR spectra, the chemical shifts for the $SiMe_3$ protons are found to be very sensitive to cobalt

(18) Falloon, S. B.; Szafert, S.; Arif, A. M.; Gladysz, J. A. *Chem.*−*Eur. J.* **1998**, *4*, 1033.

(19) (a) Johnson, B. F. G.; Lewis, J.; Monari, M.; Braga, D.; Grepioni, F. *J. Organomet. Chem.* **1989**, *377*, C1. (b) Deeming, A. J.; Manning, P. J. *Philos. Trans. R. Soc. London Ser. A* **1982**, *308*, 59.

(20) (a) Constable, E. C.; Johnson, B. F. G.; Lewis, J.; Paine, G. N.; Taylor, M. J. *J. Chem. Soc., Chem. Commun.* **1982**, *754*. (b) Holmgren, J. S.; Shapley, J. R.; Belmonte, P. A. *J. Organomet. Chem.* **1985**, *284*, C5.

(21) Zuno-Cruz, F. J.; Carrasco, M. J.; Rosales-Hoz, M. *Polyhedron* **2002**, *21*, 1105.

Table 1. $\Delta\delta+$ and $\Delta\delta-$ Values for Complexes 3−8

compound	$\Delta\delta+$	$\Delta\delta-$
3 (⊥)	203.3	67.3
6 (⊥)	257.9	69.7
5 (ll)	271.7	68.9
4	225.8	74.0
7	224.0	73.4
8	234.0	54.6

complexation on the adjacent alkyne bond. As expected, the NMR spectra show significant downfield shifts for $SiMe_3$ in the Co_2-functionalized complexes **3**−**7** by ca. 0.13 and 0.20 ppm with respect to the free ligand, in accordance with the reduction in the C≡C triple-bond character.[22] For all dmpm and dppm complexes the diastereotopic protons of the $-CH_2-$ group are coupled with the two chemically unequivalent P atoms; thus they appear as a double triplet with *J* values of ca. 13.6 and ca. 3.3 Hz (see Experimental Section).

The ^{31}P spectra, at room temperature, of all compounds **3**−**7** always show a broad singlet that is shifted to higher frequencies (ca. 10 and 35 ppm for the dmpm and dppm complex, respectively) with respect to the free ligands because of the coordination.

The ^{13}C NMR chemical shifts of the different types of carbonyl groups in all the complexes were assigned by comparison with those of the parent compounds (**1**, **2**, or **8**−**10**) and appear as two groups of signals at around δ 199−206 ppm for cobalt-carbonyls and δ 198−190 and 172−160 ppm for ruthenium- and osmium-carbonyls, respectively, suggesting that they are rapidly interchanging on the NMR scale. ^{13}C chemical shifts for similar compounds appear at higher fields in osmium complexes than in the ruthenium one. The ^{13}C NMR resonances of the coordinated acetylene units were easily identified, and the chemical shifts of the carbon centers of the Co_2C_2 cluster cores give rise to triplet resonances, with J_{CP} values of ca.11 Hz, in the range of analogous complexes (δ 74−100 ppm).[16c,18,20] The unambiguous assignment (see Experimental Section) of all carbon atoms has been carried out by using heteronuclear two-dimensional correlation spectroscopy (HMBC and HMQC).

^{13}C NMR data for acetylide **3** and **6**, for parallel **5**, and for edge-bridged **4** and **7** are included in the Experimental Section. The assignments for both C_α and C_β are based on data in the literature and appear in the range reported by Carty et al.[23] The spectra show that the chemical shifts for C_α are found downfield from those of C_β.

The chemical shifts of $C_\alpha$and C_β should be affected directly by the electron-donating ability of alkyne or acetylide substituents and the presence of substituents on the cluster frame; therefore, depending on the metal and the substituent, their chemical shifts change. It has been proposed that changes in the chemical shifts (δ) of the acetylide carbons may be associated with a change in their charges, although the observed chemical shifts are also dominated by paramagnetic terms of the screening constants. Further, it was proposed that the sum $\delta(C_\alpha) + \delta(C_\beta) = (\Delta\delta+)$ reflects the total charge alteration in the triple bond, while the difference $\delta(C_\alpha) - \delta(C_\beta) = (\Delta\delta-)$ can be used as a measure of the polarization of that bond.[23,24] These $\Delta\delta+$ and $\Delta\delta-$ are summarized in Table 1. $\Delta\delta-$ values show only slight differences from each other. This suggests that the polarization of the C≡C bond is similar in these compounds.

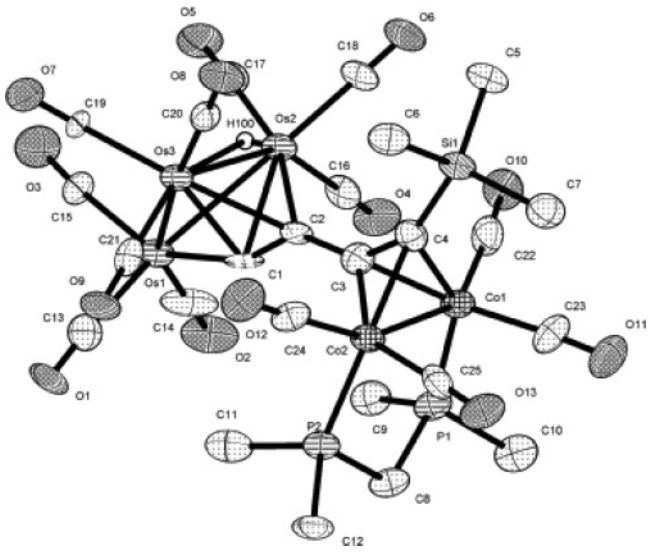

Figure 1. ORTEP diagram of **3**. H atoms have been removed for clarity.

$\Delta\delta+$ values reflect that the total charge alteration in the triple bond is higher in complex **5** with a μ_3-η^2 parallel mode.

Shifts for both C_α and C_β appear in the range reported by Carty et al.[23,16c] The chemical shifts for C_α move to lower fields, as in all μ_3-η^2 species,[23] in the sequence acetylides < edge-bridge < parallel. The chemical shifts for C_β remain relatively unchanged in **4** and **7**, where C_β is uncoordinated to the metal, while in **3** and **5** a small shift is observed compared with the parent compound **1**. These tendencies show how the electron densities of the two acetylene carbon atoms are altered separately due to complexation to the transition metals. This contrasting trend means that in these complexes the C_α and C_β quaternary carbon atoms must have a significantly different degree and mode of interaction with the Os atoms. Deshielding of C_α can probably be attributed to the development of a positive charge density on this atom due to coordination to electrophilic $M(CO)_n$ fragments. A metal effect on the C_α shifts is observed with a higher upfield shift in Os than in Ru.

The different types of carbonyl groups in complexes **3**, **5**, and **6** were assigned by comparison with those reported for similar complexes.[23] At room temperature only b, d, and e Co can be observed.

The NMR spectroscopic data (^1H, ^{31}P, and ^{13}C) for complexes **3**−**7** are consistent with the overall geometry established in the solid state for complexes **3**, **6**, and **7** (Figures 1−3), with the IR spectroscopy studies, and with the proposed structures (Scheme 1).

All compounds gave satisfactory mass spectral data; thus the positive FAB mass spectra show the respective molecular ions or $M^+ - CO$, as well as peaks corresponding to the consecutive loss of the CO ligands.

X-ray Crystallography. The single-crystal X-ray structures of complexes **3**, **6**, and **7** (Figures 1−3) confirm those presented in Scheme 1. The selected geometric parameters for these complexes have been summarized in Table 2. Compounds **3** and **6** crystallize in the triclinic crystal system, space group $P\bar{1}$, with two molecules in the asymmetric unit. The molecular structures (Figures 1 and 2) confirm the μ_3-η^1:η^2 (⊥) coordination mode of the acetylide unit, C(1)−C(2), C(26)−C(27), to the triangular Os_3 and Ru_3 cluster. Only the μ-H atom bridging Os(2)−Os(3) was located in the structural determination. The metallic atoms define a nearly equilateral triangle. The Os and

(22) Harris, R. K. *Nuclear Magnetic Resonance Spectroscopy: A Physiochemical View*; Pitman: London, 1983.

(23) Carty, A. J.; Cherkas, A. A.; Randall, L. H. *Polyhedron* **1988**, *7*, 1045.

(24) Gervasio, G.; Gobetto, R.; King, P. J.; Marabello, D.; Sappa, E. *Polyhedron* **1998**, *17*, 2937.

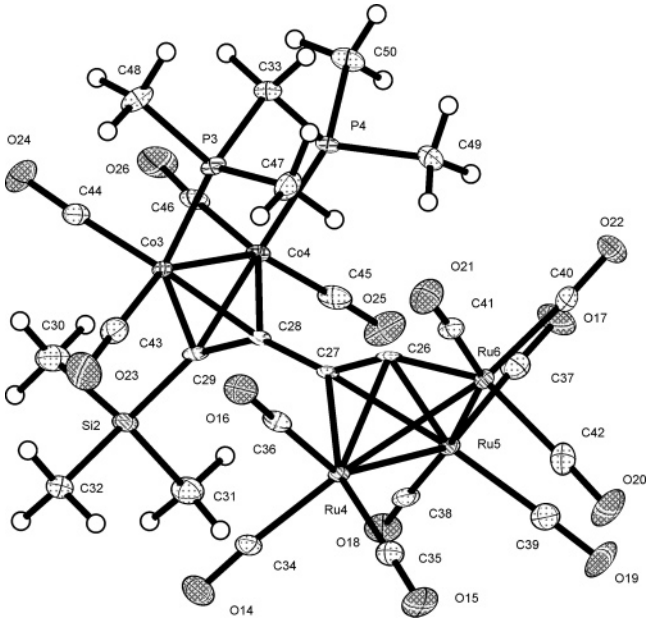

Figure 2. ORTEP diagram of **6**. H atoms have been removed for clarity.

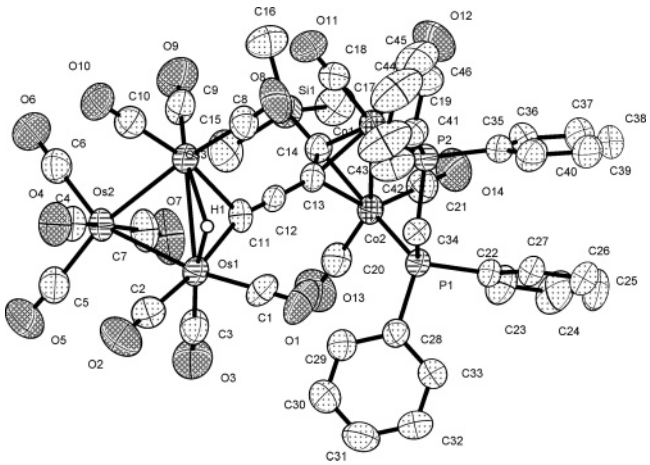

Figure 3. ORTEP diagram of **7**. H atoms have been removed for clarity.

Ru atoms are each linked to three terminal carbonyl ligands, which are essentially linear.

In **3** and **6** the torsion angles C(1)−C(2)−C(3)−C(4) and C(26)−C(27)−C(28)−C(29) are −178.8(18)°, −175.1(19)° and −178.6(5)°, −179.3(5)°, respectively. The torsion angles Co(1)−Co(2)/Os(2)−Os(3) and Co(3)−Co(4)/Os(4)−Os(6) in **3** and Co(1)−Co(2)/Ru(2)−Ru(3), Co(3)−Co(4)/Ru(4)−Ru(5) in **6** are 176.30°, 178.80° and 178.86°, 176.23° respectively; that is, the two metal−metal bonds in both complexes are essentially parallel.[13d] In these complexes the total deviation of the C_4 chain from linearity is 102°, 96.5° (**3**) and 92.8°, 94.1° (**6**).

The geometry of the $Co_2(CO)_4$dmpm fragment coordinated to the C−C triple bond is normal. The Co−C distances in the Co_2C_2 core of **3** and **6** range from 1.949(14) to 1.993(14) and from 1.967(4) to 1.989(4) Å, respectively, and these distances show in both complexes an asymmetric pattern, as observed in [{$Co_2(CO)_6(\mu$-η^2-HC≡C)}$_2$(C_6H_4)].[25] The Co_2C_2 tetrahedron is distorted with the longer Co−C interaction being associated with the alkylenic carbon coordinated to the Si atom of the trimethylsilyl group. Other structural details are similar to those for analogous complexes.[26]

In **6** we have found and modeled disorder in the carbon atoms of the dppm ligand. The atoms involved in this disorder are C(8), C(23), and C(24), and for all of them the occupancy factors have been fixed to 0.5. In all the figures this disorder has been omitted for clarity.

Compound **7** crystallizes in the monoclinic crystal system space group *C*2/*c*. The molecular structure is depicted in Figure 3. The Os(3)−C(12) distance (3.031 Å) is well beyond the normal bonding range, and so, the $Co_2(\mu$-η^2-Me_3SiC_2C≡C)(μ-dppm)$(CO)_4$ fragment coordinates to the Os_3 cluster in the μ-η^1 mode, and both the carbon atom and the hydride ligand bridge the Os(1) and Os(3) atoms. The distances Os(3)−C(11), 2.233 Å, and Os(1)−C(11), 2.120 Å, together with the bond angles C(12)−C(11)−Os(3), 120°, and C(12)−C(11)−Os(1), 160°, seem to indicate that the alkyne ligand, through C(11), contributes more than one electron to the Os_3 cluster.[16a] This will be reinforced by the electrochemical study (next section). The Os(1)−Os(2) and Os(2)−Os(3) bond distances are normal: 2.842(3) and 2.839(3) Å, respectively. The Os(1)−Os(3) bond is slightly shorter: 2.789(3) Å. The Os(1) and Os(3) atoms are each linked to three terminal carbonyl ligands, and the Os(2) atom is bonded to four carbonyl ligands with Os−CO lengths in the range 1.897(7)−1.955(7) Å. The Os−C−O angles are in the range 175.4(7)−179.6(7)°. To our knowledge only the analogous complexes of rhenium [(η^5-C_5Me_5)Re(NO)(PPh_3)-(μ-η^1-CC)$_n$$Os_3(CO)_{10}$H] ($n$ = 1, 2, 3) have been previously reported,[18] and in this case, when n = 1, the Re−C and Re−C−C bond lengths indicate contributions of both ReC≡C$(Os)_3$ and $^+$Re=C=C=$(Os)_3^-$ resonance forms.

The dicobalt unit is coordinated to a C−C triple bond in the usual manner. The lengths of the Co−Co bond (2.485(12) Å) and the coordinated triple bond (1.365(8) Å) are similar to the values in complexes **3** and **6** (Table 2) and are analogous to those previously reported for bridging alkyne ligands in $Co_2(CO)_6$ and $Co_2(CO)_4$(dppm) complexes.[8e,13d,26−28] The Co−C distances in the Co_2C_2 core range from 1.974(5) to 1.984(5) Å, and these distances do not show an asymmetry pattern.

Angles at the carbon atom chains [C(11)−C(12)−C(13) 178.1(6)°, C(12)−C(13)−C(14) 142.9(5)°, C(13)−C(14)-Si(1) 148.7(4)°] indicate the expected bending occurring on coordination to the Co_2 core. The total deviation from the linearity is 70.3°, smaller than in **3** and **6**, as expected from the different coordination mode of the acetylide group to these trimetallic clusters.

Electrochemistry. Compounds **1** and **2** contain no Os_3 or Ru_3 unit. Their electrochemical behavior was described elsewhere[26] and will be employed here in order to assign and discuss the different electrochemical features found in the mixed Co−Os or Co−Ru (**3**−**7**) compounds. Cyclic and square-wave voltammetry (CV and SWV) measurements were carried out for **1**−**7**. $E_{1/2} = (E_{pa} + E_{pc})/2$ values were determined by both techniques in the case of reversible waves; for irreversible peaks, E_p data correspond to SWV.

The electrochemical oxidations of all the mixed compounds Co−Os (**3**−**5**, **7**) or Co−Ru (**6**) show a first monoelectronic

(25) Housecroft, C. E.; Johnson, B. F. G.; Khan, M. S.; Lewis, J.; Raithby, P. R.; Robson, M. E. *J. Chem. Soc., Dalton Trans*. **1992**, 3171.

(26) Macazaga, M. J.; Marcos, M. L.; Moreno, C.; Benito-Lopez, F.; Gomez-González, J.; González-Velasco, J.; Medina, R. M. *J. Organomet. Chem.* **2006**, *691*, 138.

(27) Kunz, H.; Haldmann, H. *Comprehensive Organometallic Chemistry* II; Abel, E. W., Stone, F. G. A., Wilkinson, G., Eds.; Elsevier: New York, 1995.

(28) Arnanz, A.; Marcos, M. L.; Moreno, C.; Farrar, D. H.; Lough, A. J.; Yu, J. O.; Delgado, S.; González-Velasco, J. *J. Organomet. Chem*. **2004**, *689*, 3218.

Table 2. Selected Bond Lengths [Å], Angles [deg], and Torsion Angles [deg] for 3, 6, and 7

Compound **3**

C(1)−C(2)	1.364(19)	C(27)−Os(4)	2.309(13)
C(1)−Os(1)	1.960(14)	C(27)−Os(6)	2.326(14)
C(1)−Os(3)	2.242(13)	C(28)−C(29)	1.34(2)
C(1)−Os(2)	2.244(11)	C(28)−Co(4)	1.956(15)
C(2)−C(3)	1.408(19)	C(28)−Co(3)	1.976(14)
C(2)−Os(3)	2.314(13)	C(29)−Co(3)	1.982(13)
C(2)−Os(2)	2.338(12)	C(29)−Co(4)	1.993(13)
C(3)−C(4)	1.36(2)	Co(1)−Co(2)	2.479(3)
C(3)−Co(1)	1.949(14)	Co(3)−Co(4)	2.485(3)
C(3)−Co(2)	1.957(15)	Os(1)−Os(2)	2.8329(10)
C(4)−Co(1)	1.975(15)	Os(1)−Os(3)	2.8387(9)
C(4)−Co(2)	1.993(14)	Os(2)−H(100)	1.12(13)
C(26)−C(27)	1.35(2)	Os(2)−Os(3)	2.8347(9)
C(26)−Os(5)	1.954(14)	Os(3)−H(100)	2.58(14)
C(26)−Os(4)	2.207(13)	Os(4)−Os(6)	2.8334(8)
C(26)−Os(6)	2.248(11)	Os(4)−Os(5)	2.8361(9)
C(27)−C(28)	1.40(2)	Os(5)−Os(6)	2.8335(8)
C(1)−C(2)−C(3)	139.9(12)	C(26)−C(27)−C(28)	142.5(13)
C(4)−C(3)−C(2)	143.3(14)	C(29)−C(28)−C(27)	146.0(14)
C(3)−C(4)−Si(1)	154.8(12)	C(28)−C(29)−Si(2)	155.0(12)
C(1)−C(2)−C(3)−C(4)	−178.8(18)	C(26)−C(27)−C(28)−(29)	−175.1(19)

Compound **6**

Ru(1)−C(1)	1.947(4)	Co(1)−C(3)	1.970(4)
Ru(1)−Ru(3)	2.7947(4)	Co(1)−C(4)	1.987(4)
Ru(1)−Ru(2)	2.7997(4)	Co(1)−Co(2)	2.4799(9)
Ru(2)−C(1)	2.195(4)	Co(2)−C(3)	1.967(4)
Ru(2)−C(2)	2.303(4)	Co(2)−C(4)	1.989(4)
Ru(2)−Ru(3)	2.7968(4)	Co(3)−C(28)	1.970(4)
Ru(3)−C(1)	2.202(4)	Co(3)−C(29)	1.980(4)
Ru(3)−C(2)	2.309(4)	Co(3)−Co(4)	2.4787(8)
Ru(4)−C(26)	2.198(4)	Co(4)−C(28)	1.976(4)
Ru(4)−C(27)	2.294(4)	Co(4)−C(29)	1.983(4)
Ru(4)−Ru(5)	2.7990(4)	C(1)−C(2)	1.315(5)
Ru(4)−Ru(6)	2.8027(4)	C(3)−C(4)	1.357(5)
Ru(5)−C(26)	2.201(3)	C(26)−C(27)	1.305(5)
Ru(5)−C(27)	2.337(4)	C(27)−C(28)	1.428(5)
Ru(5)−Ru(6)	2.7948(4)	C(28)−C(29)	1.356(5)
Ru(6)−C(26)	1.946(4)		
C(1)−C(2)−C(3)	145.2(4)	C(26)−C(27)−C(28)	145.4(4)
C(4)−C(3)−C(2)	146.5(4)	C(29)−C(28)−C(27)	146.2(4)
C(3)−C(4)−Si(1)	155.5(3)	C(28)−C(29)−Si(2)	154.3(3)
C(1)−C(2)−C(3)−C(4)	−178.6(5)	C(26)−C(27)−C(28)−(29)	−179.3(5)

Compound **7**

C(11)−C(12)	1.214(7)	C(14)−Co(2)	1.977(5)
C(11)−Os(1)	2.129(6)	C(14)−Co(1)	1.984(5)
C(11)−Os(3)	2.233(6)	Co(1)−Co(2)	2.4852(12)
C(12)−C(13)	1.393(7)	Os(1)−Os(3)	2.7893(3)
C(13)−C(14)	1.365(8)	Os(1)−Os(2)	2.8420(3)
C(13)−Co(2)	1.974(5)	Os(2)−Os(3)	2.8396(3)
C(13)−Co(1)	1.977(5)	Os(3)−H(1)	2.18(9)
C(14)−Si(1)	1.847(6)	Os(1)−H(1)	1.630(9)
C(12)−C(11)−Os(1)	160.3(5)	C(14)−C(13)−C(12)	142.9(5)
C(12)−C(11)−Os(3)	120.2(5)	C(14)−C(13)−Co(2)	69.9(3)
C(11)−C(12)−C(13)	178.1(6)	C(13)−C(14)−Si(1)	148.7(4)
C(11)−C(12)−C(13)−(14)	−104(18)		

chemically reversible wave in the +0.52 to +0.82 V vs Fc^{*+}/Fc* potential range (Fc* = decamethylferrocene; see Experimental Section) (Figures 4−6). The $E_{1/2}$ value (Table 3) and voltammetric characteristics allow us to unambigously assign this peak to the removal of one electron from a molecular orbital centered in the Co_2C_2 redox unit. The peak intensity (i_P) of this wave linearly depends on $\upsilon^{1/2}$ (υ = sweep rate; 0.05 to 20 V/s range), as corresponds to a diffusion-controlled process.

The most positive $E_{1/2}$(ox) value (0.82 V) is found for the dppm-substituted **7**, as expected regarding the less donating character of this phosphine ligand as compared to dmpm, present in all remaining complexes **3**−**6**. The latter makes the Co_2C_2 core more electron-rich and, consequently, easier to oxidate. The influence of phosphine basicity agrees with previously studied compounds.[6g,h,26,28]

In dmpm-substituted compounds, the influence of the presence of the Os_3 or Ru_3 cluster on the $E_{1/2}$ value for the oxidation of the Co_2C_2 center is strikingly small, except in the case of **5**, in which $E_{1/2}$ = 0.52 V is significatively less positive than for the model compound **1** ($E_{1/2}$ = 0.70 V) and the mixed compounds **3**, **4**, and **6**. The coordination of the Os_3 cluster in **5** is in the parallel mode, and $E_{1/2}$ results indicate that this mode influences the π-character of the bridging ligand, probably shortening the C−C distance between the two central C atoms.

Although the effect is clearly smaller, the opposite is observed for **4**, with an edge-bridged-coordinated Os_3 cluster: $E_{1/2}$ for **4** is more positive than for the model compound **1** (0.76 vs 0.70 V).

When the anodic sweep is extended beyond the completely reversible Co_2C_2 oxidation peak, all the mixed **3**−**7** compounds

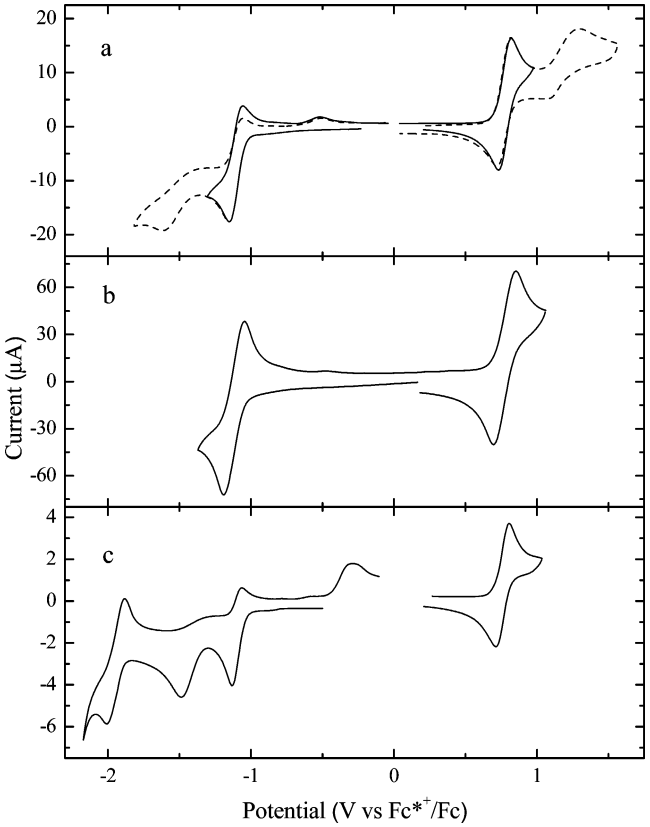

Figure 4. Cyclic voltammograms for the reduction and oxidation of **4** in CH_2Cl_2 solution containing 0.2 M $TBAPF_6$: (a) at 25 °C and $\upsilon = 0.1$ V/s on Pt; (b) at 25 °C and $\upsilon = 2$ V/s on Pt; at −30 °C and $\upsilon = 0.1$ V/s on C working electrode. Dashed lines correspond to measurements with extended potential limits.

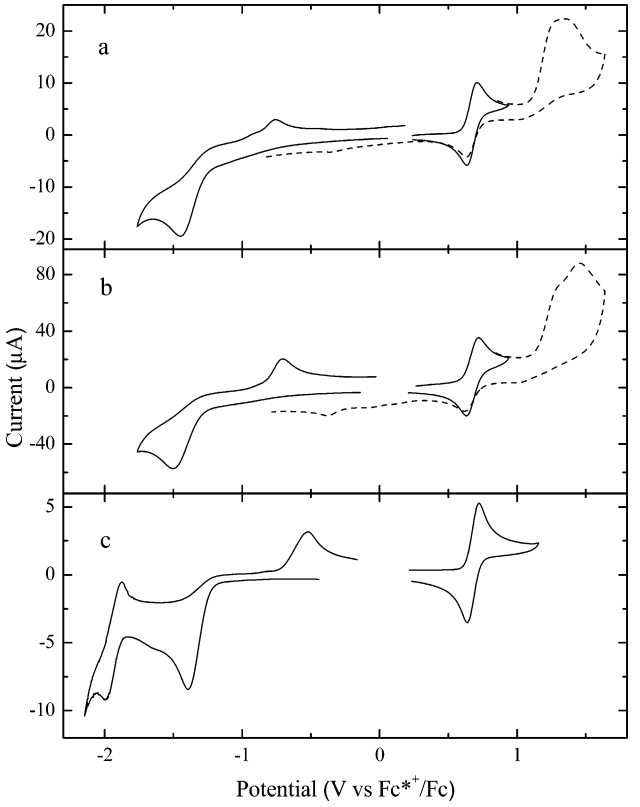

Figure 5. Cyclic voltammograms for the reduction and oxidation of **6** in CH_2Cl_2 solution containing 0.2 M $TBAPF_6$: (a) at 25 °C and $\upsilon = 0.1$ V/s on Pt; (b) at 25 °C and $\upsilon = 1$ V/s on Pt; at −30 °C and $\upsilon = 0.1$ V/s on C working electrode. Dashed lines correspond to measurements with extended potential limits.

exhibit completely irreversible oxidations in the +1.10 to +1.29 V potential range (Figures 4−6). The complete absence of these peaks in the models **1** and **2** indicates that the new features are due to Os_3/Ru_3-centered oxidations. Neither compound showed any kind of chemical reversibility for this peak, even at high sweep rates or low temperature (−30 °C), which indicates that the resulting cations are involved in fast homogeneus chemical reactions in solution.

The reduction behavior of **3**−**7** strongly depends on the coordination mode of the Os_3 or Ru_3 cluster. The edge-bridged compounds **4** and **7** show a first reduction wave at about −1.1 V, which is completely chemically reversible for $\upsilon > 1$ V/s at 25 °C or at all sweep rates at −30 °C (Figure 4). The peak intensity of this reversible wave is almost equal to that of the oxidation wave of the Co_2C_2 core, which indicates it corresponds to a one-electron reduction. At the same time, the potential value (ca. −1.1 V) is much less negative than the reduction potential of the Co_2C_2 center in **1** and **2** (−1.70 V). Therefore, the wave at −1.10 V can be assigned to the addition of one electron in a molecular orbital centered in the neutral Os_3 cluster to achieve a chemically stable species. This electrochemical result seems to indicate that the alkyne ligand can be regarded as a two-electron donor through C(11). Thus the neutral Os_3 cluster seems to have a 47-electron configuration.

The reversible reduction in **4** and **7** is followed by an irreversible peak at −1.53 V, which very probably corresponds to a further reduction (and decomposition) of the Os_3 center. When temperature is lowered to −30 °C and the sweep is extended up to quite negative values, a new chemically reversible monoelectronic peak appears at about −1.90 V. According to $E_{1/2}$ and voltammetric characteristics, this must correspond to the reduction of the redox center Co_2C_2 of the species, resulting from the homogeneous reaction after the cathodic process at −1.53 V. The dppm-substituted redox center is reduced at a slightly less negative potential (−1.88 V) than the dmpm-substituted (−1.94 V), as expected due to the more donating character of dmpm.

Perpendicularly Os_3- and Ru_3-coordinated **3** and **6** exhibit a different reduction behavior. The cathodic scan shows a first completely irreversible wave at −1.36 and −1.20 V, respectively (Figure 5). On sweep reversal, products originated by anion decomposition reoxidate at ca. −0.64 V. Os_3 complex **3** is further reduced at −1.68 V (irreversible). As found for **4** and **7**, both **3** and **6** show a monoelectronic completely chemically reversible (at −30 °C) wave at a very negative potential (−1.92 V for both) due to the Co_2C_2 remaining redox center.

The reduction behavior of **5** (parallel-coordinated Os_3 cluster) also shows a first completely irreversible wave a −1.20 V followed by a monoelectronic chemically reversible (at −30 °C) wave at −1.97 V (Figure 6). The latter must be due to the remaining Co_2C_2 center, in accordance with the rest of the compounds.

Experimental Section

General Procedures. All reactions and manipulations were routinely carried out by using standard Schlenk[29] vacuum-line and syringe techniques under an atmosphere of oxygen-free Ar or N_2. All solvents for synthetic use were reagent grade. Hexane was dried and distilled over sodium in the presence of benzophenone under

(29) Shriver, D. F.; Drezdzon, M. A. *The Manipulation of Air-Sensitive Compounds*, 2nd ed.; Wiley: New York, 1986.

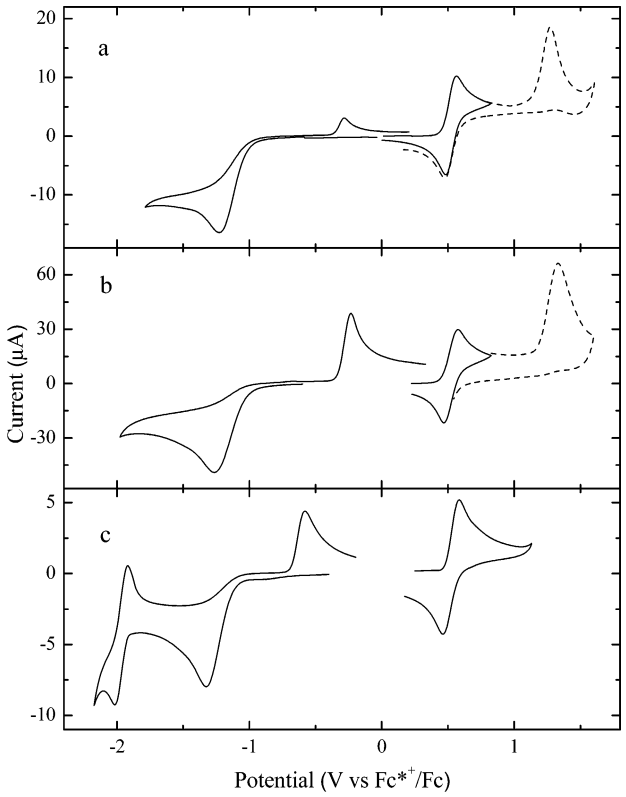

Figure 6. Cyclic voltammograms for the reduction and oxidation of **5** in CH_2Cl_2 solution containing 0.2 M $TBAPF_6$: (a) at 25 °C and $\upsilon = 0.1$ V/s on Pt; (b) at 25 °C and $\upsilon = 1$ V/s on Pt; at −30 °C and $\upsilon = 0.1$ V/s on C working electrode. Dashed lines correspond to measurements with extended potential limits.

Table 3. Electrochemical Data[a] for 1−7

	$E_{1/2}$ (red)			$E_{1/2}$ (ox)		
1			−1.70	+0.70		
2			(*−1.70*)	(*+0.75*)		
3	−1.36[b]	−1.68[b]	−1.92	+0.68	+1.29[b]	
4	−1.10	−1.53[b]	−1.94	+0.76	+1.14[b]	
5	−1.20[b]		−1.97	+0.52	+1.24[b]	
6	−1.20[b]		−1.92	+0.67	+1.12[b]	
7	−1.07	−1.53[b]	−1.88	+0.82	+1.10[b]	+1.40[b]

[a] In V vs Fc^{*+}/Fc^* in CH_2Cl_2 solution (values in italics are in THF solution). Data are taken from CV and SWV at 25 and −30 °C. [b] E_p in SWV of irreversible peak.

an Ar atmosphere. Also under Ar, CH_2Cl_2 was dried and distilled over CaH_2, Na, and $MgSO_4$, respectively. All solvents were bubbled with Ar for 1 h after distillation and then stored under Ar or degassed by means of at least three freeze−pump−thaw cycles after distillation and before use. Column chromatography was performed by using silica gel 100 (Fluka) and preparative TLC on 20 × 20 cm glass plates coated with silica gel (SDS 60−17 μm, 0.25 mm thick). $Co_2(CO)_8$, HC≡CSiMe$_3$, 1,4-bis(trimethylsilyl)butadiyne (Me$_3$SiC≡CC≡CSiMe$_3$), triruthenium dodecacarbonyl, triosmium dodecacarbonyl (Fluka), 1,2-bis(dimethylphosphino)methane (Strem), 1,2-bis(diphenylphosphino)methane, and tetrabutylamonium fluoride (Bu_4NF) (Aldrich) were used as received. Trimethylamine *N*-oxide (Me_3NO) (Fluka) was sublimed prior to use and stored under Ar. The compounds [$Co_2(\mu$-η^2-HC≡CC$_2$SiMe$_3$)(μ-dmpm)(CO)$_4$][6i] (**1**), [$Co_2(\mu$-η^2-HC≡CC$_2$SiMe$_3$)(μ-dppm)(CO)$_4$][6h] (**2**), [$Os_3(CO)_{10}$(MeCN)$_2$], and [$Ru_3(CO)_{10}(MeCN)_2$][17] were prepared according to literature procedures and characterized by their IR and NMR spectra. The ^{1}H, ^{13}C, ^{31}P, and proton-decoupled ^{31}P NMR spectra and HMQC (heteronuclear multiple quantum correlation) and HMBC (heteronuclear multiple bond correlation) experiments were recorded on Bruker AMX-300 and -500 instruments. Chemical shifts were measured relative either to an internal reference of tetramethylsilane or to residual protons of the solvents. Infrared spectra were measured on a Perkin-Elmer 1650 infrared spectrometer. Elemental analyses were performed by the Microanalytical Laboratory of the University Autónoma of Madrid on a Perkin-Elmer 240 B microanalyzer. Electronic spectra were recorded on a Unicam UV 4 UV−visible spectrophotometer. Mass spectra were measured on a VG-Autospec mass spectrometer for FAB by the Mass Laboratory of the University Autónoma of Madrid. Electrochemical measurements were carried out with a computer-driven Par model 273 electrochemistry system in a three-electrode cell under N_2 atmosphere in anhydrous deoxygenated solvents (CH_2Cl_2 and THF) containing 0.2 M tetrabutylammonium hexafluorophosphate ($TBAPF_6$) as supporting electrolyte. Cyclic and square-wave voltammetry (CV and SWV, respectively) studies were carried out. Polycrystalline Pt (0.05 cm^2) or glassy carbon were used as working electrodes; the counter electrode was a Pt gauze and the reference electrode was a silver wire quasi-reference electrode. Decamethylferrocene (Fc*) was used as internal standard, and all potentials in this work are referred to the Fc^{*+}/Fc^* couple. Under the actual experimental conditions, $E_{1/2}$ of the ferrocene couple (Fc^+/Fc) was +0.44 V vs Fc^{*+}/Fc^* in THF solution and +0.55 V vs Fc^{*+}/Fc^* in CH_2Cl_2 solution.

Reaction of [$Co_2(\mu$-η^2-HC≡CC$_2$SiMe$_3$)(μ-dmpm)(CO)$_4$] (1) with [$Os_3(CO)_{10}(MeCN)_2$]. A mixture of **1** (0.21 g, 0.44 mmol) and [$Os_3(CO)_{10}(MeCN)_2$] (0.40 g, 0.44 mmol) in CH_2Cl_2 (50 mL) was stirred at room temperature for 26 h. The reaction was monitored by FTIR ^{1}H NMR and TLC. The reaction was stopped when all the starting material had been consumed. After removal of solvent under vacuum, the residue was eluted with CH_2Cl_2 on a silica column and then purified by thin-layer chromatography (TLC) using hexane/CH_2Cl_2 (3:1). Three bands were eluted to afford [Os_3-(μ-H){μ_3-η^1:η^2;μ-η^2-C$_2$C$_2$SiMe$_3$[Co_2(μ-dmpm)(CO)$_4$]}(CO)$_9$] (**3**) (15% yield), [Os_3(μ-H){μ-η^1;μ−η^2-C$_2$C$_2$SiMe$_3$[Co_2(μ-dmpm)-(CO)$_4$]}(CO)$_{10}$] (**4**) (52% yield), and [Os_3{μ_3-η^1:η^2;μ−η^2-HC$_2$C$_2$-SiMe$_3$[Co_2(μ-dmpm)(CO)$_4$]}(μ-CO)(CO)$_9$] (**5**) (33% yield) as stable yellow-brown solids. **3** has also been obtained as the only product in high yield (97%) from thermal decomposition of **5**.

Compound 3: red-brown solid. IR (CH_2Cl_2, cm^{-1}): ν_{CO} 2096.1 (m), 2072.1 (vs), 2047.8 (vs), 2020.2 (vs), 1987.8 (m), 1961.8 (m). ^{1}H NMR (300 MHz, $CDCl_3$, ppm): δ 2.99 (dt, $J_{HH} = 10.4$ Hz, $J_{PH} = 13.6$ Hz, 1H, P−CH$_2$−P), 2.33 (dt, $J_{HH} = 10.5$ Hz, $J_{PH} = 13.6$ Hz, 1H, P−CH$_2$−P); 1.60 (t, $J_{PH} = 3.3$ Hz, 6H, −PMe), 1.56 (t, $J_{PH} = 3.6$ Hz, 6H, −PMe); 0.41 (s, 9H, Me$_3$SiC−); −22.02 (s, 1H, μ-H). ^{31}P NMR (121 MHz, $CDCl_3$, ppm): δ 10.1 (s br, 2P). ^{13}C NMR (125 MHz, CD_2Cl_2, ppm): δ 206.8 (m, Co−CO), 203.9 (m, Co−CO); 172.2 (s, Os−CO), 170.4 (s, Os−CO); 164.9 (s, Os−CO); 135.2 (s, C$_4$), 92.4 (t, C$_2$), 84.6 (t, C$_1$); 68.0 (s, C$_3$); 43.9 (t, $J_{CP} = 22.0$ Hz, P−CH$_2$−P); 21.0 (t, $J_{CP} = 13.4$ Hz, Me), 18.2 (t, $J_{CP} = 15.7$ Hz, Me); 2.3 (s, Me$_3$SiC−). MS (FAB$^+$, *m/z*): 1311.9 (M$^+$); 1283.9 (M$^+$ − CO); 1255.9 (M$^+$ − 2CO); 1227.9 (M$^+$ − 3CO); 1199.9 (M$^+$ − 4CO); 1171.9 (M$^+$ − 5CO); 1143.9 (M$^+$ − 6CO); 1115.9 (M$^+$ − 7CO); 1087.9 (M$^+$ − 8CO); 1059.9 (M$^+$ − 9CO); 1031.9 (M$^+$ − 10CO). Anal. Calc for $C_{25}H_{24}O_{13}Co_2Os_3P_2Si$: C, 22.9; H, 1.8. Found: C, 22.7; H, 2.1.

Compound 4: dark red-brown solid. IR (CH_2Cl_2, cm^{-1}): ν_{CO} 2101.8 (m), 2062.0 (vs), 2054.5 (s), 2017.5 (vs), 2004.5 (vs), 1976.8 (s). ^{1}H NMR (300 MHz, $CDCl_3$, ppm): δ 2.61 (dt, $J_{HH} = 10.8$ Hz, $J_{PH} = 13.5$ Hz, 1H, P−CH$_2$−P), 2.27 (dt, $J_{HH} = 10.4$ Hz, $J_{PH} = 13.6$ Hz, 1H, P−CH$_2$−P); 1.62 (t, $J_{PH} = 3.3$ Hz, 6H, −PMe), 1.55 (t, $J_{PH} = 3.7$ Hz, 6H, −PMe); 0.36 (s, 9H, Me$_3$SiC−); −15.83 (s, 1H, μ-H). ^{31}P NMR (121 MHz, $CDCl_3$, ppm): δ 10.7 (s br, 2P). ^{13}C NMR (125 MHz, CD_2Cl_2, ppm): δ 205.4 (m, Co−CO), 201.8 (m, Co−CO); 182.8 (d, $J_{CH} = 17.3$ Hz Os−CO), 180.4 (s, Os−CO), 177.2 (s, Os−CO), 172.9 (d, $J_{CH} = 9.0$ Hz Os−CO), 171.7 (s, Os−CO); 149.9 (s, C$_4$), 93 (t, C$_1$), 75.9 (s, C$_3$), 74.0 (t, C$_2$); 42.4 (t, $J_{CP} = 21.4$ Hz, P−CH$_2$−P); 20.7 (t, $J_{CP} = 13.0$ Hz, Me),

18.8 (t, J_{CP} = 16.7 Hz, Me); 1.35 (s, Me_3SiC-). MS (FAB$^+$, *m/z*): 1339.7 (M^+); 1311.7 ($M^+ - CO$); 1283.7 ($M^+ - 2CO$); 1255.7 ($M^+ - 3CO$); 1227.7 ($M^+ - 4CO$); 1199.7 ($M^+ - 5CO$); 1171.7 ($M^+ - 6CO$); 1143.7 ($M^+ - 7CO$); 1115.7 ($M^+ - 8CO$) 1087.7 ($M^+ - 9CO$). Anal. Calc for $C_{26}H_{24}O_{14}Co_2Os_3P_2Si$: C, 23.3; H, 1.8. Found: C, 23.1; H, 2.1.

Compound 5: yellow solid. IR (CH_2Cl_2, cm^{-1}): ν_{CO} 2096.3 (m), 2061.0 (vs), 2050.9 (vs), 2021.6 (s), 1994.4 (s), 1950.4 (m). ^{1}H NMR (300 MHz, $CDCl_3$, ppm): δ 8.78 (s, 1H, C≡C−H); 2.19 (m, 2H, P−CH_2−P); 1.54 (t, J_{PH} = 2.7 Hz, 6H, −PMe), 1.45 (t, J_{PH} = 3.5 Hz, 6H, −PMe); 0.30 (s, 9H, Me_3SiC-). ^{31}P NMR (121 MHz, $CDCl_3$, ppm): δ 12.8 (s br, 2P). ^{13}C NMR (125 MHz, CD_2Cl_2, ppm): δ 182.3 (m, Os−CO), 178.1 (m, Os−CO); 170.3 (s, C_4), 101.4 (s, C_3), 96.2 (t, C_1), 86.6 (t, C_2); 43.1 (t, J_{CP} = 20.2 Hz, P−CH_2−P); 20.9 (t, J_{CP} = 12.4 Hz, Me), 19.7 (t, J_{CP} = 17.3 Hz, Me); 2.1 (s, Me_3SiC-). MS (FAB$^+$, *m/z*): 1339.1 (M^+); 1311.1 ($M^+ - CO$); 1283.1 ($M^+ - 2CO$); 1255.1 ($M^+ - 3CO$); 1227.1 ($M^+ - 4CO$); 1199.1 ($M^+ - 5CO$); 1171.1 ($M^+ - 6CO$); 1143.1 ($M^+ - 7CO$); 1115.1 ($M^+ - 8CO$); 1087.1 ($M^+ - 9CO$). Anal. Calc for $C_{26}H_{24}O_{14}Co_2Os_3P_2Si$: C, 23.3; H, 1.8. Found: C, 23.0; H, 2.0.

Reaction of [Co_2(μ-η^2-HC≡CC_2SiMe_3)(μ-dmpm)(CO)$_4$] with [$Ru_3(CO)_{10}(MeCN)_2$] or [$Ru_3(CO)_{12}$]. Complex **1** (0.15 g, 0.31 mmol) and [$Ru_3(CO)_{10}(MeCN)_2$] or [$Ru_3(CO)_{12}$] (0.19 g, 0.31 mmol) were dissolved in CH_2Cl_2/MeCN (50 mL). The brownish-yellow solution was stirred at room temperature, and the reaction was monitored by FTIR, ^{1}H NMR, and TLC. After 48 h the solvent was removed under vacuum, and the product was purified by thin-layer chromatography (TLC) using hexane/CH_2Cl_2 (1:1) or by a hexane-packed silica column (200 g) using the same eluent to afford the stable brown-yellow solid **6** (80% yields).

Compound 6: brown-yellow solid. IR (CH_2Cl_2, cm^{-1}): ν_{CO} 2092.6 (m), 2068.0 (vs), 2048.5 (vs), 2017.6 (vs), 1986.4 (s), 1959.3 (m). ^{1}H NMR (300 MHz, $CDCl_3$, ppm): δ 3.05 (dt, J_{HH} = 11.0 Hz, J_{PH} = 13.6 Hz, 1H, P−CH_2−P), 2.36 (dt, J_{HH} = 10.6 Hz, J_{PH} = 13.6 Hz, 1H, P−CH_2−P); 1.62 (t, J_{PH} = 3.3 Hz, 6H, −PMe), 1.57 (t, J_{PH} = 3.7 Hz, 6H, −PMe); 0.39 (s, 9H, Me_3SiC-); −19.79 (s, 1H, μ-H). ^{31}P NMR (121 MHz, $CDCl_3$, ppm): δ 9.19 (s br, 2P). ^{13}C NMR (125 MHz, CD_2Cl_2, ppm): δ 206.8 (m, Co−CO), 204.0 (m, Co−CO); 197.9 (s, Ru−CO), 189.6 (s, Ru−CO); 163.8 (s, C_4), 94.1 (s, C_3), 92.0 (t, C_2), 84.9 (t, C_1); 44.1 (t, J_{CP} = 20.5 Hz, P−CH_2−P), 21.5 (t, J_{CP} = 13.5 Hz, Me), 18.4 (t, J_{CP} = 15.7 Hz, Me); 1.35 (s, Me_3SiC-). MS (FAB$^+$, *m/z*): 1043.8 (M^+); 1015.8 ($M^+ - CO$); 987.8 ($M^+ - 2CO$); 959.8 ($M^+ - 3CO$); 931.8 ($M^+ - 4CO$); 903.8 ($M^+ - 5CO$); 875.8 ($M^+ - 6CO$); 847.8 ($M^+ - 7CO$); 819.8 ($M^+ - 8CO$); 791.8 ($M^+ - 9CO$); 763.8 ($M^+ - 10CO$); 735.8 ($M^+ - 11CO$). Anal. Calc for $C_{25}H_{24}O_{13}Co_2Ru_3P_2Si$: C, 28.8; H, 2.3. Found: C, 28.5; H, 2.5.

Reaction of [Co_2(μ-η^2-HC≡CC_2SiMe_3)(μ-dppm)(CO)$_4$] (2) with [$Os_3(CO)_{10}(MeCN)_2$]. The same procedure as described above was followed in the preparation of [Os_3(μ-H){μ-η^1;μ-η^2-$C_2C_2SiMe_3$-[Co_2(μ-dppm)(CO)$_4$]}(CO)$_{10}$], **7**, from **2** (0.20 g, 0.27 mmol) and [$Os_3(CO)_{10}(MeCN)_2$] (0.27 g, 0.30 mmol). After 24 h the solvent was removed under vacuum, and the product was purified by thin-layer chromatography (TLC) using hexane/CH_2Cl_2 (3:1). Two bands were eluted. The faster-moving yellow band contained minor amounts of [$Os_3(CO)_{10}(MeCN)_2$]; the slower-moving dark red band gave **7** (0.35 g, 91% yields).

Compound 7. IR (CH_2Cl_2, cm^{-1}): ν_{CO} 2101.9 (m), 2063.4 (vs), 2055.1 (sh), 2032.3 (m), 2019.1 (vs) 2010.3 (vs) 1983.1 (s). ^{1}H NMR (300 MHz, $CDCl_3$, ppm): δ 7.41 (m, 8H, *o*-Ph); 7.33 (m, 12H, *m*-, *p*-Ph); 3.52 (m, 2H, P−CH_2−P); 0.38 (s, 9H, −$SiMe_3$); −15.73 (s, 1H, μ-H). ^{31}P NMR (121 MHz, $CDCl_3$, ppm): δ 31.71 (s br, 2P). ^{13}C NMR (125 MHz, $CDCl_3$, ppm): δ 204.7 (m, Co−CO); 201.2 (m, Co−CO); 182.1 (s, Os−CO), 181.3 (s, Os−CO), 179.6 (s, Os−CO), 176.6 (s, Os−CO), 171.7 (s, Os−CO), 171.3 (s, Os−CO); 148.7 (s, C_4); 136.8 (t, J_{CP} = 22.9 Hz, *i*-Ph); 134.4 (t, J_{CP} = 17.4 Hz, *i*-Ph); 132.0 (t, J_{CP} = 5.9 Hz, *o*-Ph); 131.06 (t, J_{CP} = 6.4 Hz, *o*-Ph); 129.9 (s, *p*-Ph); 128.8 (t, J_{CP} = 5.0 Hz, *m*-Ph); 128.1 (t, J_{CP} = 5.0 Hz, *m*-Ph); 96.1 (t, C_1); 75.3 (s, C_3); 70.6 (s, C_2); 1.04 (s, −$SiMe_3$). MS (MALDI, *m/z*): 1587.8 [M^+]; 1559.3 [$M^+ - 1$ CO]; 1531.8 [$M^+ - 2$ CO]; 1503.6 [$M^+ - 3$ CO]; 1475.4 [$M^+ - 4$ CO]; 1447.3 [$M^+ - 5$ CO]; 1419.8 [$M^+ - 6$ CO]; 1391.8 [$M^+ - 7$ CO]; 1363.8 [$M^+ - 8$ CO]; 1335.8 [$M^+ - 9$ CO]; 1307.8 [$M^+ - 10$ CO]; 1279.8 [$M^+ - 11$ CO]; 1251.7 [$M^+ - 12$ CO]. Anal. Calc for $C_{46}H_{32}O_{14}Co_2Os_3P_2Si$: C, 34.8; H, 1.9. Found: C, 34.5; H, 2.2.

Reaction of HC≡$CSiMe_3$ with [$Os_3(CO)_{10}(MeCN)_2$]. The same procedure as described above was followed in this reaction from HC≡$CSiMe_3$ (0.025 g, 0.27 mmol) and [$Os_3(CO)_{10}(MeCN)_2$] (0.25 g, 0.27 mmol). After 24 h the solvent was removed under vacuum, and the product was purified by thin-layer chromatography (TLC) using hexane/CH_2Cl_2 (3:1). Three bands were eluted. The two faster-moving yellow bands contained the new edge-bridged complex [Os_3(μ-H){μ-η^1-$C_2SiMe_3(CO)_{10}$] (**8**) and a minor amounts of [Os_3(μ-H){μ_3-η^1:η^2-$C_2SiMe_3(CO)_9$] (**9**); the slower-moving yellow band gave [Os_3(μ_3-η^1:η^2-HC_2SiMe_3(μ-CO)$(CO)_9$] (**10**) (0.18 g, 71% yields). This method essentially corresponds to published preparative procedures.[30]

Compound 8. IR (CH_2Cl_2, cm^{-1}): ν_{CO} 2110.0 (m), 2060.5 (vs), 2050.0 (s), 2019.5 (vs), 2006.5 (vs), 1978.8 (s). ^{1}H NMR (300 MHz, $CDCl_3$, ppm): δ 0.39 (s, 9H, Me_3SiC-); −16.9 (s, 1H, μ-H). ^{13}C NMR (125 MHz, $CDCl_3$, ppm): δ 182.0 (s, CO); 174.2 (s, CO); 172.4 (s, CO); 169.5 (s, CO); 144.3 (s, C_α); 89.7 (s, C_β); 0. 0.5 (s, −$SiMe_3$).

X-ray Crystallography. Red crystals of **3**, **6**, and **7** were obtained by recrystallization of the complexes from CH_2Cl_2/hexane mixtures. A summary of selected crystallographic data for these complexes is given in Table 4. Different single crystals with prismatic shape and approximate dimensions of 0.07 × 0.04 × 0.02 mm (**3**), 0.09 × 0.06 × 0.04 mm **(6)**, and 0.10 × 0.03 × 0.02 mm (**7**) were mounted on glass fibers and transferred to a Bruker SMART 6K CCD area-detector three-circle diffractometer with a MAC Science Co., Ltd. rotating anode (Cu Kα radiation, λ = 1.54178 Å) generator equipped with Goebel mirrors at settings of 50 kV and 110 mA.[31] X-ray data were collected at 273, 100, and 297 K for **3**, **6**, and **7**, respectively, with a combination of six runs at different φ and 2θ angles, 3600 frames. The data were collected using 0.3° wide ω scans (15 s/frame at 2θ = 40° and 30 s/frame at 2θ = 100°), with a crystal-to-detector distance of 4.0 cm.

The raw intensity data frames were integrated with the SAINT program,[32] which also applied corrections for Lorentz and polarization effects.

The substantial redundancy in data allows empirical absorption corrections (SADABS)[33] to be applied using multiple measurements of symmetry-equivalent reflections. A total of 22 715 (**3**), 28 206 (**6**), and 31 217 (**7**) reflections were collected and 11 949 (**3**), 11 472(**6**), and 9388 (**7**) independent reflections remained after merging R(int) = 0.0524, $R(\sigma)$ = 0.1250 (**3**), R(int) = 0.0297, $R(\sigma)$ = 0.0740 (**6**), and R(int) = 0.0326, $R(\sigma)$ = 0.0798 (**7**).

The software package SHELXTL version 6 × 10[34] was used for space group determination, structure solution, and refinement. The structure was solved by direct methods (SHELXS-97),[35] completed with difference Fourier syntheses, and refined with full-

(30) Johnson, B. F. G.; Lewis, J.; Monari, M.; Braga, D.; Grepioni, F. *J. Organomet. Chem*. **1989**, *377*, C1.

(31) *SMART* v. 5.625, Area-Detector Software Package; Bruker AXS: Madison, WI, 1997−2001.

(32) *SAINT+ NT* ver. 6.04, SAX Area-Detector Integration Program; Bruker AXS: Madison, WI, 1997−2001.

(33) Sheldrick, G. M. *SADABS* version 2.03, a Program for Empirical Absorption Correction; Universität Göttingen, 1997−2001.

(34) Bruker AXS *SHELXTL* version 6.10, Structure Determination Package; Bruker AXS: Madison, WI, 2000.

(35) Sheldrick, G. M. *SHELXS-97*, Program for Structure Solution. *Acta Crystallogr*. *Sect. A* **1990**, *46*, 467.

Table 4. Crystal Data and Structure Refinement for 3, 6, and 7

	3	6	7
empirical formula	$C_{50}H_{48}Co_4O_{26}Os_6P_4Si_2$	$C_{50}H_{48}Co_4O_{26}P_4Ru_6Si_2$	$C_{46}H_{32}Co_2Os_3P_2Si$
fw	2621.86	2086.98	1587.21
temperature	273(2) K	100(2) K	297(2) K
wavelength	1.54178 Å	1.54178 Å	1.54178 Å
cryst syst	triclinic	triclinic	monoclinic
space group	$P\bar{1}$	$P\bar{1}$	$C2/c$
unit cell dimens	$a = 12.3334(4)$ Å $b = 17.6257(5)$ Å $c = 18.0899(5)$ Å $\alpha = 70.163(2)°$ $\beta = 79.042(2)°$ $\gamma = 78.187(2)°$	$a = 12.34170(10)$ Å $b = 17.6232(2)$ Å $c = 18.1300(2)$ Å $\alpha = 70.2550(10)°$ $\beta = 78.9300(10)°$ $\gamma = 78.0460(10)°$	$a = 31.7835(7)$ Å $b = 11.8192(3)$ Å $c = 27.0178(6)$ Å $\alpha = 90°$ $\beta = 95.4220(10)°$ $\gamma = 90°$
volume	3589.58(18) Å^3	3598.92(6) Å^3	10104.0(4) Å^3
Z	2	2	8
density (calcd)	2.425 Mg/m^3	1.914 Mg/m^3	2.087 Mg/m^3
absorp coeff	28.276 mm^{-1}	18.699 mm^{-1}	20.265 mm^{-1}
$F(000)$	2414	2006	5968
cryst size	0.07 × 0.04 × 0.02 mm^3	0.09 × 0.06 × 0.04 mm^3	0.10 × 0.03 × 0.02 mm^3
θ range for data collection	2.62 to 70.57°	2.61 to 66.23°	2.79 to 70.57°
index ranges	$-14 \le h \le 14$, $-21 \le k \le 20$, $-20 \le l \le 20$	$-12 \le h \le 14$, $-20 \le k \le 18$, $-20 \le l \le 21$	$-35 \le h \le 38$, $-14 \le k \le 13$, $-31 \le l \le 32$
no. of reflns collected	22 715	22 806	31 217
no. of indep reflns	11 949 [R(int) = 0.0618]	11 472 [R(int) = 0.0316]	9388 [R(int) = 0.0496]
completeness to $\theta = 62.63°$	86.9%	90.9%	96.9%
absorp corr	semiempirical from equivalents	semiempirical from equivalents	empirical
max. and min. transmn			0.544 and 0.341
refinement method		full-matrix least-squares on F^2	
no. of data/restraints/params	11 949/0/835	11 472/668/850	9388/0/620
goodness-of-fit on F^2	0.966	1.024	1.017
final R indices [$I > 2\sigma(I)$]	R1 = 0.0524, wR2 = 0.1250	R1 = 0.0297, wR2 = 0.0740	R1 = 0.0326, wR2 = 0.0798
R indices (all data)	R1 = 0.0829, wR2 = 0.1412	R1 = 0.0327, wR2 = 0.0757	R1 = 0.0428, wR2 = 0.0855
largest diff peak and hole	3.670 and −1.919 e Å^{-3}	1.267 and −1.184 e Å^{-3}	1.214 and −1.057 e Å^{-3}

matrix least-squares using SHELXL-97[36] minimizing $w(F_o^2 - F_c^2)$.[2] Weighted R factors (R_w) and all goodness of fit S are based on F^2; conventional R factors (R) are based on F. All non-hydrogen atoms were refined with anisotropic displacement parameters. All hydrogen atoms were fixed at geometric positions. All scattering factors and anomalous dispersions factors are contained in the SHELXTL 6.10 program library.

Final positional parameters, anisotropic thermal parameters, and structure amplitudes are available as Supporting Information.

CCDC-620822, -620823, and -620825 contain the supplementary crystallographic data for this paper. These data can be obtained free of charge from The Cambridge Crystallographic Data Centre via www.ccdc.cam.ac.uk/data_request/cif.

Acknowledgment. We express our great appreciation to the Dirección General de Investigación Científica y Tecnológica (Grant No. CTQ2006-10940/BQU), Spain.

Supporting Information Available: CIF files giving further details of the crystal structure determination (compounds **3**, **6**, and **7**), including bond lengths, bond angles, and anisotropic and isotropic displacement parameters. This material is available free of charge via the Internet at http://pubs.acs.org.

OM700525Z

(36) Sheldrick, G. M. *SHELXL-97*, Program for Crystal Structure Refinement; Universität Göttingen, 1997.